

Metalloocene–nucleobase conjugates. Synthesis, structure and nucleic acid binding

Clayton Price, Mehmet Aslanoglu, Christian J. Isaac, Mark R. J. Elsegood, William Clegg, Benjamin R. Horrocks* and Andrew Houlton*[†]

Department of Chemistry, University of Newcastle upon Tyne, Newcastle upon Tyne NE1 7RU, UK

The ferrocenylnucleobase conjugates $[\text{Fe}(\eta^5\text{-C}_5\text{H}_5)\{\eta^5\text{-C}_5\text{H}_4\text{CH}_2\text{NMe}_2\text{CH}_2\text{CH}_2\text{CH}_2\text{-NC(O)NHC(O)CMeCH}_3\}][\text{BF}_4]$ **1** and $[\text{Fe}(\eta^5\text{-C}_5\text{H}_5)\{\eta^5\text{-C}_5\text{H}_4\text{CH}_2[\text{C}_5\text{H}_2\text{N}_4(\text{NH}_2)]\}]$ **2** of thymine and adenine respectively, have been prepared and their crystal and molecular structures determined. The molecular packing of the two compounds differs markedly in terms of intermolecular hydrogen-bonding interactions. In **1** such interactions are confined to discrete cation \cdots anion \cdots solvate units, whereas in **2** the hydrogen-bonding patterns are extensive and involve both the Watson–Crick and Hoogsteen donor and acceptor sites. Electrochemical studies of the interaction of **1** with nucleic acids showed that the incorporation of this single nucleoside base with the metallocene moiety enhances the binding in aqueous solution compared to a cationically charged derivative devoid of this functionality. Moreover, with immobilised nucleic acid, binding was observed exclusively for the conjugate **1**.

As an area of bioorganometallic chemistry, studies of the interaction of organometallic compounds with nucleic acids have primarily focused on metallation reactions with nucleotide bases.^{1–5} This is due, largely, to the reported antitumour activity of metallocene dihalides, with apparent localisation of the metal-containing species in the cell nucleus.^{6,7}

Iron-containing sandwich compounds are also known to display antitumour activity despite the apparent lack of vacant co-ordination sites.^{7–12} As a consequence, the mode of action for this class of compounds may involve non-covalent interactions with cellular targets such as nucleic acids. Such interactions would be expected to be modified by the functionalities attached to the ferrocenyl group. The extensive substitution chemistry of ferrocene provides considerable scope for the design of organometallic derivatives capable of non-covalent binding to nucleic acids and other key cellular targets.

In addition to potential therapeutic applications, due to their near ideal electrochemical behaviour, ferrocenyl derivatives capable of recognising DNA are also anticipated to be useful in analytical applications.^{13,14} While electrochemically active DNA-binding agents have been developed, these have generally been based on co-ordination compounds^{15,16} and organic derivatives.¹⁷

For application in this area the advantages of using immobilised nucleic acids have been recognised and various approaches have been developed. These range from adsorption on simple oxidised metal surfaces¹⁸ to self-assembled molecular-based structures.¹⁹ The combination of these immobilisation methods and electrochemically active DNA-binding agents can then exploit the sensitivity of adsorptive-transfer cyclic voltammetry, a technique which has been demonstrated as a viable strategy for biosensor design.¹⁶ Very recently the synthesis of redox-active 5'-ferrocenyl-3'-thiol modified oligonucleotides, which are capable of self-immobilisation onto a gold surface, has elegantly combined these approaches.²⁰

In an effort to exploit these potential analytical and therapeutic applications we have initially prepared metallocenes functionalised with nucleobases. Ferrocenyl derivatives func-

tioned in this way may be capable of interacting with nucleic acids *via* hydrogen-bonding interactions as well as acting as substrate analogues for enzymatic systems such as ribonucleotide reductase and other nucleoside-binding proteins.²¹

Here we report the preparation and crystal and molecular structures of ferrocenyl-based nucleoside analogues containing thymine and adenine. We also report electrochemical studies on the binding of one such compound with nucleic acids both in solution and with nucleic acids immobilised on a chemically modified surface. The results demonstrate that the conjugation of a single nucleobase to the ferrocenyl moiety can influence the binding to nucleic acids.

Results and Discussion

Synthesis

The compound $[\text{Fe}(\eta^5\text{-C}_5\text{H}_5)\{\eta^5\text{-C}_5\text{H}_4\text{CH}_2\text{NMe}_2\text{CH}_2\text{CH}_2\text{-CH}_2\text{NC(O)NHC(O)CMeCH}_3\}][\text{BF}_4]$ **1** was prepared by reaction of 1-(3-bromopropyl)thymine and *N,N*-dimethylaminomethylferrocene in methanol. The crude product was converted into the tetrafluoroborate salt and crystals suitable for X-ray crystallographic analysis were obtained from methanol. The compound $[\text{Fe}(\eta^5\text{-C}_5\text{H}_5)\{\eta^5\text{-C}_5\text{H}_4\text{CH}_2\text{-[C}_5\text{H}_2\text{N}_4(\text{NH}_2)]\}]$ **2** was prepared by refluxing an aqueous solution of *N,N,N*-trimethylammoniomethylferrocene iodide with adenine as described elsewhere.²² The crude material was chromatographed on a silica column. Crystals suitable for X-ray analysis were obtained by slow cooling of a dimethylformamide (dmf) solution.

Crystal and molecular structures of compounds **1** and **2**

Table 1 presents crystallographic data and other information, Table 2 selected structural parameters for compounds **1** and **2**, and Figs. 1 and 2 show the molecular structure and numbering schemes used in each case. All bond lengths and angles are typical from comparison with analogous compounds.²³

In compound **1** the iron–ring distances are ≈ 1.64 and ≈ 1.66 Å for the substituted and unsubstituted cyclopentadienyl rings, respectively. The interplanar angle between the rings is 5.1° and

[†] E-mail: andrew.houlton@newcastle.ac.uk

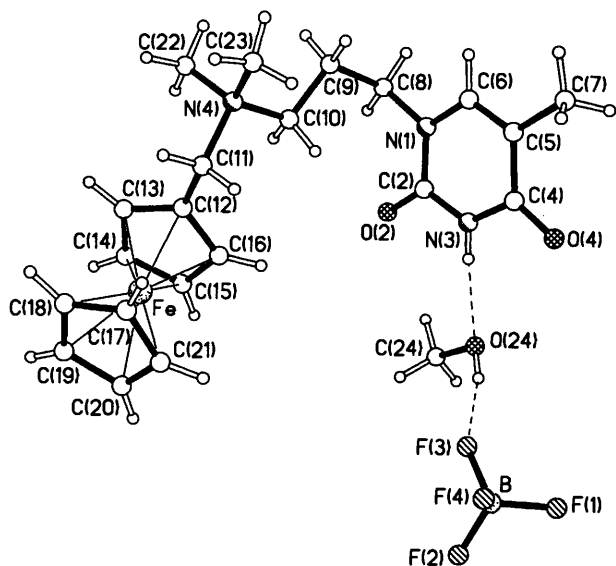


Fig. 1 Molecular structure of compound 1 showing the atomic numbering scheme and the hydrogen bonding

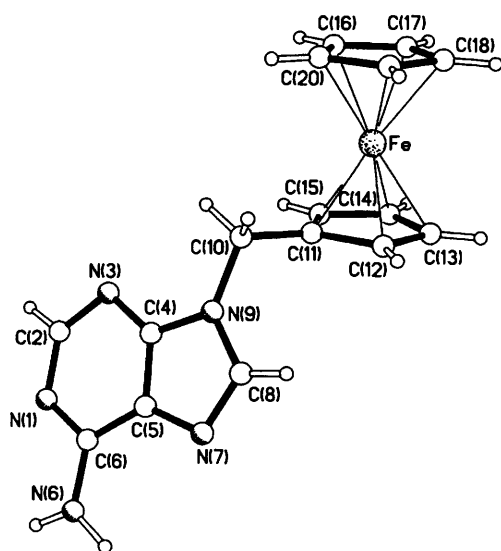


Fig. 2 Molecular structure of compound 2 showing the atomic numbering scheme

that between the substituted ring and thymine group is 38.0° . The C–N bond lengths to the quaternised nitrogen range from 1.496(5) (average) for the $\text{CH}_3\text{–N}$ distance to 1.552(5) Å for the $\text{C}_5\text{H}_4\text{CH}_2\text{–N}$ bond length. The occluded methanol is involved in hydrogen bonding of the imide NH group of thymine to the oxygen of MeOH ($\text{N}\cdots\text{O}$ distance 2.828 Å, $\text{N–H}\cdots\text{O}$ 176°). Further hydrogen bonding is seen between the solvent and BF_4^- anion ($\text{O}\cdots\text{F}$ distance 2.860 Å, $\text{O–H}\cdots\text{F}$ angle 163°). Hydrogen bonding does not propagate through the crystal structure but is confined to these discrete units.

Comparison with the crystal structure of 1-methylthymine²⁴ is instructive and potentially relevant to the binding studies discussed herein. The structure consists of layers of extended hydrogen-bonded sheets. These intermolecular interactions occur primarily between dimers with $\text{N}\cdots\text{O}$ distance of 2.830 Å and an $\text{N–H}\cdots\text{O}$ angle of 167° . These dimers are weakly associated through a $\text{C–H}\cdots\text{O}$ interaction (3.113 Å, $\text{C–H}\cdots\text{O}$ 166°).

Compound 1 crystallises in the centrosymmetric space group $P2_1/n$. Inversion centres generate a stack comprising parallel ferrocenyl groups on the exterior of the stack and thymine moieties on the inside. This gives rise to a pseudo-helix structure

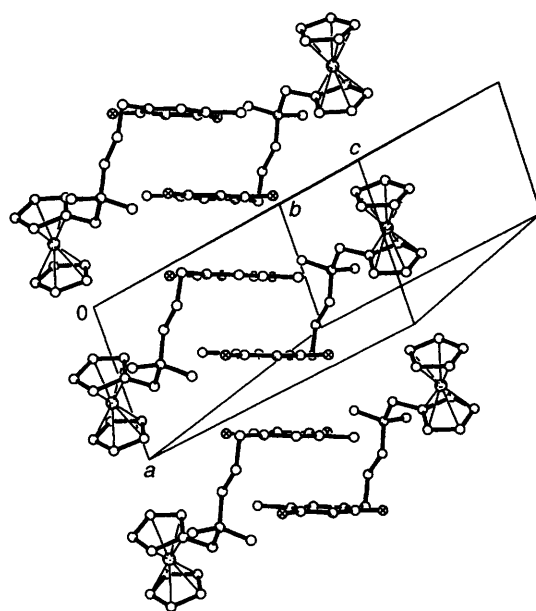


Fig. 3 Stacking interactions of the cations in the crystal structure of compound 1

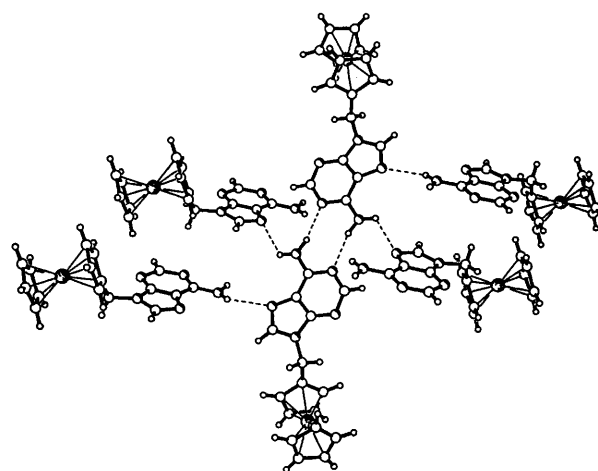


Fig. 4 Hydrogen-bonding interactions involving the adenine of compound 2. Each adenine interacts with three others utilising donor and acceptor sites involved in Watson–Crick and Hoogsteen type base pairings

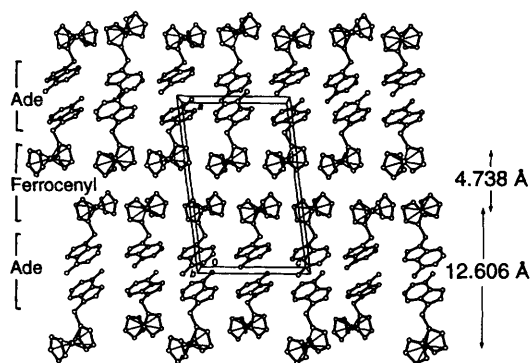
throughout the crystal lattice. The shortest intrastack $\text{Fe}\cdots\text{Fe}$ distance is 7.215 Å (the *a*-axis length) and the intrastack cyclopentadienyl ring distance is ≈ 3.2 Å. The thymine groups are parallel within the stack and the intrastack spacing between adjacent groups is alternately 3.344 and 3.370 Å (Fig. 3).

In compound 2 the ferrocenylmethyl cation is bonded directly to N(9) of adenine (Fig. 2). The $\text{Fe–C}_5\text{H}_5$ distance is ≈ 1.65 Å compared to ≈ 1.64 Å for the substituted ring. The interplanar angle between the rings is 0.9° and that between the substituted ring and the adenine group is 115.1° . The C–N bond length for the $\text{C}_5\text{H}_4\text{CH}_2\text{–N}$ linkage is significantly shorter at 1.470(5) Å than that in 1, reflecting the change in hybridisation at nitrogen from sp^3 to sp^2 in the two compounds.

Extensive hydrogen bonding is observed throughout the crystal lattice of compound 2. The adenine moieties are hydrogen bonded *via* a Watson–Crick type pairing, involving N(1) and HN(6) generating centrosymmetric dimers [$\text{N}(3)\cdots\text{N}(1)$ 3.115 Å, $\text{N–H}\cdots\text{N}$ 166° , Fig. 4]. The remaining amino proton interacts with N(7) on an adjacent molecule [$\text{N}(6)\cdots\text{N}(7)$ 3.026 Å, $\text{N–H}\cdots\text{N}$ 122.4°]. In this way each adenine group interacts through hydrogen bonding with three

Table 1 Crystallographic data

Compound	1	2
Formula	C ₂₁ H ₂₈ BF ₄ FeN ₃ O ₂ ·CH ₃ OH	C ₁₆ H ₁₅ FeN ₅
<i>M</i>	529.2	333.2
Crystal system	Monoclinic	Monoclinic
Space group	<i>P</i> 2 ₁ / <i>n</i>	<i>P</i> 2 ₁ / <i>c</i>
<i>a</i> /Å	7.2149(8)	17.4776(13)
<i>b</i> /Å	23.926(3)	7.2932(8)
<i>c</i> /Å	14.071(2)	11.1081(13)
β/°	101.106(2)	97.096(3)
<i>U</i> /Å ³	2383.5(5)	1405.1(2)
<i>Z</i>	4	4
<i>D</i> _c /g cm ⁻³	1.475	1.575
μ/mm ⁻¹	0.693	1.076
<i>F</i> (000)	1104	688
Crystal size/mm	0.50 × 0.39 × 0.29	0.58 × 0.18 × 0.04
Reflections for cell	7292	3125
Reflections measured	10 138	7084
Unique reflections	3941	2471
Maximum <i>h, k, l</i> indices	8, 20, 16	22, 9, 14
Reflections with <i>F</i> ² > 2σ(<i>F</i> ²)	3641	1909
<i>R</i> _{int}	0.0513	0.0606
Transmission	0.636–0.849	0.604–0.922
No. refined parameters	316	205
Weight parameters <i>a, b</i>	0.0545, 5.0408	0.0543, 1.4677
Extinction coefficient <i>x</i>	0.0019(7)	0
<i>R</i> (on <i>F</i> , observed data)	0.0635	0.0466
<i>R</i> ' = [Σ <i>w</i> (<i>F</i> _o ² - <i>F</i> _c ²)/Σ <i>w</i> (<i>F</i> _o ²) ^{1/2}]	0.1560	0.1212
Goodness of fit	1.209	1.069
Maximum, minimum electron density/e Å ⁻³	0.639, -0.764	0.618, -0.480

**Fig. 5** Molecular packing highlighting the layered structure of compound 2**Table 2** Selected bond lengths (Å) and angles (°) for compounds 1 and 2

	1	2
Fe–C (average)	2.042(4)	2.037(4)
Fe–C ₅ H ₅	1.659	1.649
Fe–C ₅ H ₄	1.640	1.638
cp–Fe–cp	5.1	0.9
C _{ipso} –C	1.485(6)	1.498(5)
C ₅ H ₄ CH ₂ –N	1.552(5)	1.470(5)
C–N(1)	1.478(5)	

cp = C₅H₄ or C₅H₅.

other adenine groups, involving all the donor and acceptor sites required for Watson-Crick and Hoogsteen base-pairing interactions, *i.e.* N(1), H₂N(6) and N(7).

Fig. 5 shows a packing diagram viewed down the *b* axis. The gross molecular packing reveals the layered nature of compound 2, which comprises discrete ferrocenyl-containing and adenine-containing regions. Each of these individual regions is double layered. Interlayer spacings between sheets of

Fe atoms are shown in Fig. 5; within a layer, closest Fe...Fe distances are 6.451, 6.851 and 7.293 Å, the Fe atoms forming an approximate hexagonal array.

A comparison with other 9-alkylated adenine derivatives reveals that compound 2 exhibits rather unusual interactions.²³ A direct comparison can be made with 9-methyladenine.²⁵ The latter structure consists of sheets comprising 9-methyladenine molecules hydrogen bonded through N(1) and H_aN(6) of one molecule interacting with N(7) and H_bN(6) of an adjacent molecule in the ribbon [N(6)...N(7) 3.074 Å, N(6)–H_b...N(7) 174°; N(6)...N(1) 2.969 Å, N(6)–H_a...N(1) 164°]. This can be described as the interaction between the Watson-Crick and Hoogsteen faces of adenine. These interactions are repeated through translational symmetry generating a polar arrangement. In contrast 8-ethyl-9-methyladenine²⁶ crystallises with Watson-Crick faces of adenine pairing as in compound 2 [N(1)...N(6) distances of 3.18 Å and an almost linear N–H...N of 171°]. However, in this case there are no further hydrogen-bonding interactions involving N(7), and the structure may be described as consisting of parallel sheets containing Watson-Crick dimer pairs.

A further survey of the Cambridge Structural Database²³ reveals few examples of ferrocenyl derivatives functionalised with nucleobases. Platinated 1-methylthymine and 1-methylcytosine derivatives of the dinuclear 1,1'-bis(diphenylphosphino)ferrocene (dppf) complex [Pt(μ-OH)(dppf)]₂[BF₄]₂ have been reported and appear to be the only examples to date.²⁷ However, in both cases the bonding to the nucleobase is *via* the platinum(II) centre.

Nucleic acid binding studies

Studies of the binding of compound 2 were not possible due to the insolubility in water.

In aqueous Tris [tris(hydroxymethyl)aminomethane] buffer at pH 7 compound 1 shows a simple, reversible one-electron oxidation typical of ferrocenes with an *E*^o value of +0.31 V vs. Ag quasi-reference electrode (QRE) and a diffusion coefficient of 2.9 × 10⁻⁶ cm² s⁻¹. The diffusion coefficients of the large nucleic acid molecules are one to two orders of magnitude

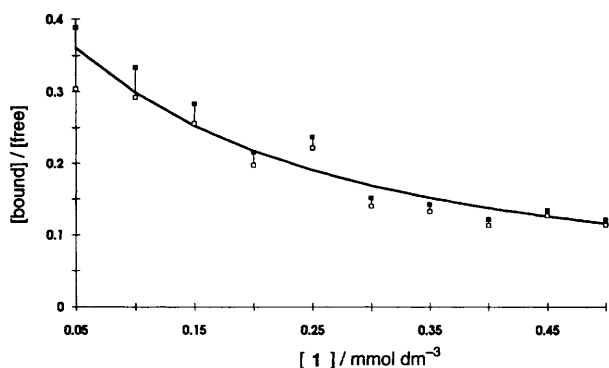


Fig. 6 Titration of compound **1** against 3.5 mmol dm^{-3} DNA (as nucleotide phosphate concentration) using a platinum-disc electrode (diameter $25 \mu\text{m}$). Plot of the ratio $[\text{bound}]/[\text{free}]$ against the total concentration of **1**. The solid line is a least-squares fit with a binding constant, $K = 6.4 \times 10^3 \text{ dm}^3 \text{ mol}^{-1}$ and $s = 25$. Error bars were calculated from an estimate of the accuracy of measurements of the steady-state current

smaller than this value and therefore a reduction in the limiting current occurs when **1** binds to these macromolecules.²⁸ This decrease in the limiting current is a direct measure of the amount of bound **1** and can be used to calculate the binding constant. Although cyclic voltammetry has been used to make similar measurements of complex–DNA interactions,^{28,29} there are advantages to the use of steady-state microelectrode voltammetry in these experiments. Since the diffusion current at a microdisc is directly proportional to the diffusion coefficient, the contribution of bound complex to the current is negligible. The diffusion current at the microdisc is therefore directly proportional to the unbound ferrocenyl concentration. This approximation was confirmed experimentally by the absence of a measurable faradaic current on irreversible binding of $[\text{Ru}(\text{NH}_3)_6]^{3+}$ to DNA until the DNA was saturated with $[\text{Ru}(\text{NH}_3)_6]^{3+}$ at which point plots of the current *vs.* $[\text{Ru}]$ in the presence and absence of DNA ran parallel.

The simplest model of the binding equilibrium is obtained by assuming each ferrocene complex binds independently and that the number of binding sites is proportional to the concentration of the nucleotide phosphate,²⁸ equation (1) where s can be

$$[\text{sites}] = [\text{NP}]/2s \quad (1)$$

interpreted as a binding-site size in terms of base pairs or as the average distance between binding sites on the nucleic acid and $[\text{NP}]$ is the concentration of nucleotide phosphate. Writing the binding constant, K , as in equation (2), where $[\text{free}]$ and $[\text{bound}]$ are the concentrations of free and bound **1**. These

$$K = [\text{bound}]/[\text{free}][\text{sites}] \quad (2)$$

were computed from the model as a function of the total complex concentration, c_T , K and s . Values of current in the absence and presence of nucleic acid were used to compute the ratio of bound to free ferrocenyl. Experimental data for the ratio $[\text{bound}]/[\text{free}]$ were fitted by the model using a standard least-squares method with K and s as the only adjustable parameters. Confidence intervals (95%) on the estimated parameters were determined by a standard Monte Carlo method.³⁰

Fig. 6 shows a typical voltammetric titration of compound **1** against DNA. The magnitude of the binding constant of **1** to RNA [$K = (1.2 \pm 0.15) \times 10^4 \text{ dm}^3 \text{ mol}^{-1}$, $s = 26 \pm 1.6$] is about twice that for DNA [$(6.4 \pm 0.4) \times 10^3 \text{ dm}^3 \text{ mol}^{-1}$, $s = 25 \pm 1.0$]. As the ionic strength was increased by adding KCl to a concentration of 20 mmol dm^{-3} the binding constant decreased. However, some residual binding was observed,

especially to RNA. We interpret this behaviour as evidence that the major contribution to the binding free energy is an electrostatic interaction, but with a minor non-electrostatic component. The binding of *N,N,N*-trimethylammoniomethylferrocene iodide to DNA was studied as a control and found to be at the limits of detection ($K \approx 10^3 \text{ dm}^3 \text{ mol}^{-1}$ in 10 mmol dm^{-3} Tris buffer, pH 7), decreasing further at higher ionic strength. This behaviour is typical of a purely electrostatic interaction between the cationic ferrocenyl derivative and the phosphate groups of DNA.

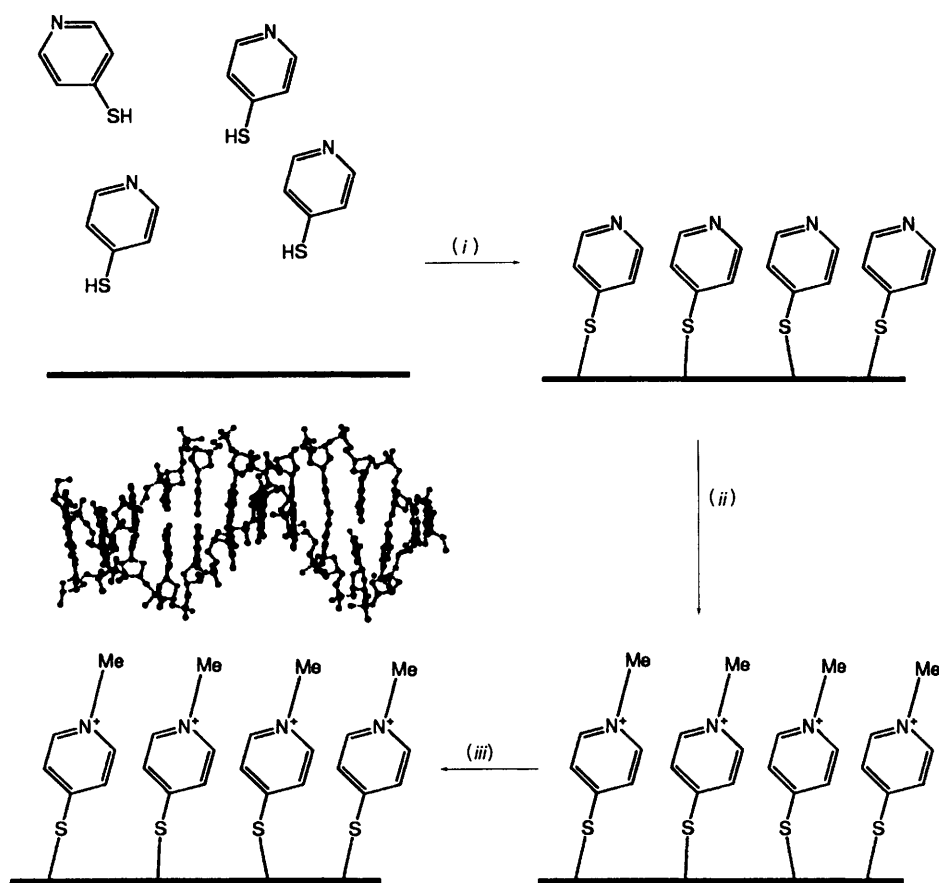
Further to investigate the binding of compound **1** with DNA, chemically modified surfaces were designed to immobilise DNA and enable us to exploit the sensitivity of adsorptive-transfer voltammetry and quartz-crystal microgravimetry (QCM). These surfaces were prepared by spontaneous adsorption of 4-sulfanylpiperidine onto Pt or Au *via* sulfur–metal bonds with subsequent methylation of the piperidine nitrogen using iodomethane to produce a cationic monolayer (Scheme 1). Following adsorption of DNA (1 h) onto these surfaces and rinsing with 10 mmol dm^{-3} Tris buffer, the electrodes were dipped into solutions of **1** in 10 mmol dm^{-3} Tris buffer (5 min). After transfer to a fresh 10 mmol dm^{-3} Tris buffer solution in the electrochemical cell surface waves at *ca.* $+0.4 \text{ V}$ (peak current proportional to scan rate, 0.2 nmol cm^{-3}) were observed for **1** (Fig. 7). No surface waves were observed in control experiments in the absence of adsorbed DNA or using *N,N,N*-trimethylammoniomethylferrocene iodide in place of **1**. The surface waves slowly decayed by about 50% over a period of roughly 30 min, which we attribute to eventual desorption of **1** and diffusion into the bulk solution. Preliminary *in-situ* gravimetric measurements using QCM showed a measurable frequency decrease (59 Hz, 0.8 nmol cm^{-2}) over a period of *ca.* 5 min on addition of a solution of **1** in 10 mmol dm^{-3} Tris buffer to a cell containing only buffer in contact with the DNA-derivatised platinum surface. The smaller coverage in the adsorptive-transfer voltammetric experiment is probably due to desorption of **1** after the transfer step. No significant frequency change ($+2 \text{ Hz}$) was observed in the control experiment with *N,N,N*-trimethylammoniomethylferrocene iodide. The adsorptive-transfer voltammetry and QCM data provide evidence for a non-electrostatic binding interaction between **1** and surface-immobilised DNA. The absence of detectable binding of *N,N,N*-trimethylammoniomethylferrocene iodide can be rationalised as a consequence of the proximity of the cationic piperidinium nitrogens in the monolayer. These data do not, however, discriminate between possible binding modes of **1** which include triplex formation with ds-DNA, or more likely a combination of hydrogen-bonding and hydrophobic effects.

Conclusion

Conjugation of a single nucleobase to a ferrocenyl derivative to give compound **1** produces a significant change in the mode of binding to nucleic acids. Steady-state microelectrode voltammetry indicated that the binding of **1** to dissolved nucleic acids is essentially electrostatic; however, adsorptive-transfer voltammetry and QCM showed that surface immobilisation of DNA can strongly influence the relative size of the electrostatic and non-electrostatic contributions to the binding free energy.

Experimental

Compound **1** was obtained from the reaction of 1-(3-bromopropyl)thymine (1 g, 4.04 mmol) with *N,N*-dimethylamino-methylferrocene (Lancaster) (0.5 g, 2.05 mmol) in methanol (50 cm^3) over 10 days. A crude product was precipitated by concentration and addition of diethyl ether. It was purified using column chromatography (matrix 60 silica), eluting with methanol–5% aqueous ammonium chloride (7:3). A yellow solid was precipitated as the tetrafluoroborate salt, by addition



Scheme 1 (i) Chemisorption of 4-sulfanylpyridine onto the metal surface; (ii) alkylation of self-assembled monolayer with 5% MeI solution; (iii) immobilisation of nucleic acid onto cationic surface

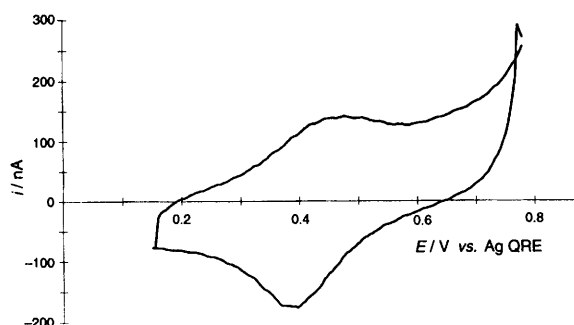


Fig. 7 Cyclic voltammogram of a 1 mm diameter gold electrode after adsorption of DNA and compound 1 followed by transfer to fresh 10 mmol dm⁻³ pH 7 Tris buffer. Sweep rate 0.1 V s⁻¹

of NaBF₄ to a concentrated solution of the columned product, yield 0.53 g (52%). ¹H NMR [(CD₃)₂SO]: δ 1.76 (s, 3 H, CH₃ of Thy), 2.06 (m, 2 H, CH₂CH₂CH₂), 2.86, [s, 6 H, N(CH₃)₂], 3.11 (t, 2 H, NCH₂C₂H₄), 3.67 [t, 2 H, CH₂NC(O)], 4.25 (s, 5 H, cyclopentadienyl H), 4.37 (s, 4 H, C₅H₄CH₂N + Cp-H's), 4.48 (s, 2 H, cyclopentadienyl H), 7.52, [s, 1 H, C(6)H] and 11.30 (s, 1 H, imide H). Crystals suitable for X-ray studies were obtained by liquid diffusion of a methanolic solution of 1 with ether.

Compound 2 was prepared as reported elsewhere.²² Crystals were grown by slow cooling of a saturated dimethylformamide solution. ¹H NMR [(CD₃)₂SO]: δ 4.14, (t, 2 H, C₅H₄), 4.19 (s, 5 H, C₅H₅), 4.37 (t, 2 H, C₅H₄), 5.09 (s, 2 H, CH₂), 7.2, (br s, 2 H, NH₂), and 8.20 (s, 2 H, CH of Ade).

X-Ray crystallography

Crystal data and other information on structure determinations

are given in Table 1. Data were measured on a Siemens SMART CCD area-detector diffractometer with graphite-monochromated Mo-K α radiation ($\lambda = 0.71073 \text{ \AA}$) at 160 K. Cell parameters were refined from angular settings of strong reflections selected from the complete data set in each case. Intensity data were measured to $\theta_{\max} = 25^\circ$ and corrected semiempirically for absorption on the basis of the high degree of redundancy and symmetry equivalence in the data. Analysis of repeated measurements showed no sign of significant intensity decay.

The structures were determined by automatic direct methods and refined on F^2 for all unique measured data, with weighting $w^{-1} = \sigma^2(F_o^2) + (aP)^2 + bP$, where $P = (F_o^2 + 2F_c^2)/3$. Hydrogen atoms were constrained with a riding model including free rotation of methyl and OH groups, and anisotropic parameters were refined for all other atoms. An isotropic extinction coefficient correction multiplies F_c by $(1 + 0.001 \times F_c^2 \lambda^3 / \sin 2\theta)^{-4}$. The final R' and goodness of fit were based on F^2 values for all data, while the conventional R was based on F values of reflections having $F_o^2 > 2\sigma(F_o^2)$, for comparison with refinements based on F . Programs: SHELXTL³¹ and local software.

Atomic coordinates, thermal parameters and bond lengths and angles have been deposited at the Cambridge Crystallographic Data Centre (CCDC). See Instructions for Authors, *J. Chem. Soc., Dalton Trans.*, 1996, Issue 1. Any request to the CCDC for this material should quote the full literature citation and the reference number 186/217.

Nucleic acid binding studies

All studies were done at room temperature (20 °C). Platinum microdisc electrodes were prepared by heat sealing platinum wire (25 or 10 μm diameter) (Goodfellow, Cambridge), in glass

tubes (outside diameter 2 mm). Electrical contact to the Pt was made *via* In/Ga eutectic and copper wire. Macroscopic platinum and gold electrodes for cyclic voltammetry were prepared by potting 1 mm diameter wires in epoxy. A silver wire was used as a quasi-reference electrode. An OxSys Micros (Oxford) low-current potentiostat was used for both cyclic voltammetry and microelectrode voltammetry. Quartz crystals (Pt-coated, area 0.196 cm²) for quartz-crystal microgravimetry were obtained from EG&G PARC for use with a QCA017 quartz-crystal microgravimeter (EG&G PARC, Reading).

Solutions of DNA (type XIV, sodium salt from herring testes, Sigma) and RNA (type XI from baker's yeast, Sigma) were prepared fresh before each experiment using doubly distilled water containing 10 mmol dm⁻³ Tris buffer adjusted to pH 7 with dilute HCl. The concentration of nucleic acid is reported as the concentration of nucleotide phosphate and determined by UV/VIS spectroscopy using a value of 6600 dm³ mol⁻¹ cm⁻¹ for the absorption coefficient.²⁸ Monolayers of 4-sulfanylpiperidine (Aldrich) were prepared by immersing gold or platinum electrodes in 1 mmol dm⁻³ ethanol solutions of the thiol for 10 min. These were methylated by immersion in 5% iodomethane in methanol for 10 min.

Acknowledgements

The Newcastle University Research Development Fund is thanked for a studentship (to C. P.), the Nuffield Foundation for a grant (to A. H.) and the Royal Society Small Equipment Fund (B. R. H.), the EPSRC for a diffractometer and a studentship (to C. J. I.) and Harran University and Higher Educational Council of Turkey for a studentship (to M. A.).

References

- 1 N. H. Agnew, T. G. Appleton, J. R. Hall, G. F. Kilmister and I. J. McMahon, *J. Chem. Soc., Chem. Commun.*, 1979, 324.
- 2 H. Bauer, G. M. Sheldrick, U. Nagel and W. Beck, *Z. Naturforsch., Teil B*, 1985, **46**, 1237.
- 3 J. H. Toney and T. J. Marks, *J. Am. Chem. Soc.*, 1985, **107**, 947; J. H. Toney, C. P. Brock and T. J. Marks, *J. Am. Chem. Soc.*, 1986, **108**, 7263.
- 4 D. P. Smith, M. T. Griffin, M. M. Olmstead, M. F. Maestro and R. H. Fish, *Inorg. Chem.*, 1993, **32**, 4677 and refs. therein.
- 5 H. Chen, M. M. Olmstead, D. P. Smith, M. F. Maestro and R. H. Fish, *Angew. Chem., Int. Ed. Engl.*, 1995, **34**, 1514.
- 6 N. Farrell, *Transition Metal Complexes as Drugs and Chemotherapeutic Agents*, Kluwer Academic Publishers, Dordrecht, 1989.
- 7 P. Köpf-Maier and H. Köpf, *Chem. Rev.*, 1987, **87**, 1137.
- 8 P. Köpf-Maier, H. Köpf and E. W. Neuse, *Angew. Chem.*, 1984, **96**, 446.
- 9 V. Scaria, A. Furlani, B. Longato, B. Corain and G. Pilloni, *Inorg. Chim. Acta*, 1988, **153**, 67.
- 10 D. T. Hill, G. R. Girard, F. L. McCabe, R. K. Johnson, P. D. Stupik, J. H. Zhang, W. M. Reiff and D. S. Eggleston, *Inorg. Chem.*, 1989, **28**, 3529.
- 11 E. W. Neuse, M. G. Meirim and N. F. Blom, *Organometallics*, 1988, **7**, 2562.
- 12 A. Houlton, R. M. G. Roberts and J. Silver, *J. Organomet. Chem.*, 1991, **418**, 107.
- 13 S. Takenaka, Y. Uto, H. Kondo, T. Ihara and M. Takagi, *Anal. Biochem.*, 1994, **218**, 436.
- 14 M. E. A. Downs, S. Kobayashi and I. Karube, *Anal. Lett.*, 1987, **20**, 437.
- 15 K. M. Millan, A. Saraullo and S. R. Mikkelsen, *Anal. Chem.*, 1994, **66**, 2943.
- 16 A. M. Pyle and J. K. Barton, *Prog. Inorg. Chem.*, 1990, **38**, 413.
- 17 S. Takenaka, T. Ihara and M. Takagi, *J. Chem. Soc., Chem. Commun.*, 1990, 1485.
- 18 H. Su, M. R. Kallury, M. Thompson and A. Roach, *Anal. Chem.*, 1994, **66**, 769.
- 19 X.-H. Xu, H. C. Yang, T. E. Mallouk and A. J. Bard, *J. Am. Chem. Soc.*, 1994, **116**, 8386.
- 20 R. C. Mucic, M. K. Herrlein, C. A. Mirkin and R. L. Letsinger, *Chem. Commun.*, 1996, 555.
- 21 L. Stryer, *Biochemistry*, W. H. Freeman, New York, 1988.
- 22 S.-C. Chen, *J. Organomet. Chem.*, 1980, **202**, 183.
- 23 F. H. Allen and O. Kennard, *Chem. Design Automation News*, 1993, **8**, 31.
- 24 K. Hoogsteen, *Acta Crystallogr.*, 1963, **16**, 28.
- 25 T. J. Kistenmacher and M. Rossi, *Acta Crystallogr., Sect. B*, 1977, **33**, 253.
- 26 S. M. Tret'yak and L. F. Sukhoub, *Z. Kristallogr.*, 1988, **22**, 772.
- 27 G. Bandoli, G. Trovo, A. Dolmella and B. Longato, *Inorg. Chem.*, 1992, **31**, 45.
- 28 M. T. Carter and A. J. Bard, *J. Am. Chem. Soc.*, 1987, **109**, 7528; *Bioconjugate Chem.*, 1990, **2**, 257.
- 29 J. Swiatek, *J. Coord. Chem.*, 1994, **33**, 191 and refs. therein.
- 30 W. H. Press, S. A. Teukolsky, W. T. Vetterling and B. P. Flannery, *Numerical Recipes in Fortran*, Cambridge University Press, 1992, ch. 15, p. 686.
- 31 G. M. Sheldrick, *SHELXTL manual*, Siemens Analytical X-ray Instruments, Madison, WI, 1994, version 5.

Received 30th May 1996; Paper 6/03758E